Electronic Supplementary Information

Chemically Suppressing Redox Reaction at NiO_x/Perovskite Interface in Narrow Bandgap Perovskite Solar Cells to Exceed Power Conversion Efficiency of 20%

Hongyu Bian[ab†], Jiayu You[a†], Cunyun Xu[a], Xiaofeng He[ab], Meng Wang[c], Yanqing Yao[d], Wenqi Zeng[ab], Pengju Guo[a], Hongyu Zhou[ab], Dengcheng Lu[a], Zhongjun Dai[ab], Sam Zhang[*ab], Qunliang Song[*a]

[a] *Institute for Clean Energy and Advanced Materials, School of Materials and Energy, Southwest University, Chongqing 400715, China.*
[b] *Center for Advanced Thin Films and Devices, School of Materials and Energy, Southwest University, Chongqing 400715, China.*
[c] *College of Materials Science and Engineering, Sichuan University, Chengdu, 610064, China.*
[d] *School of Physics and Electronic Science, Zunyi Normal College, Zunyi 563002, China.*
[*]Corresponding author.

[†] These authors contributed equally to this work.

E-mail address: samzhang@swu.edu.cn (Sam Zhang), qlsong@swu.edu.cn (QunLiang Song)

Experimental section

Materials:

Methylammonium iodide (MAI, >99.99%) and Methylammonium chloride (MACl, ≥ 99.5%) were purchased from Xi'an Polymer Light Technology Corp. Lead iodide (PbI_2, 99.99%) and formamidinium iodide (FAI, 99.9%) were purchased from Advanced Election Technology Co., Ltd. Stannous fluoride (SnF_2, 99%) was purchased from *J&K* Scientific Ltd. Tin powder (99.99%) was purchased from Meryer (Shanghai) Chemical Technology Co., Ltd. Tin iodide (SnI_2, 99.999%) was supplied from Alab (Shanghai) Chemical Technology Co., Ltd. Lead thiocyanate ($Pb(SCN)_2$) was from Sigma-Aldrich. Stannous chloride ($SnCl_2$, 99%+) was purchased from Adamas-beta. The chemical listed above composed perovskite. Ascorbic acid (AA, 99.0%), Sodium Hydroxide (NaOH, ⩾ 98%) and Nickel nitrate hexahydrate ($Ni(NO_3)_2 \cdot 6H_2O$, 99%) were received from Aladdin. All the chemicals were used without further purification unless specifically illustrated.

The solvent used in this work of *N,N*-dimethylformide (DMF) and dimethyl sulfoxide (DMSO) were bought from *J&K* Scientific Ltd. The anti-solvent, chlorobenzene (CB) used in the preparation of perovskite film was purchased from Meryer (Shanghai) Chemical Technology Co., Ltd.

Synthesis of NiO_x NPs

NiO_x NPs were synthesized according to previous report with a minor modification. 1.6 g NaOH were dissolved into 4 mL deionized water to prepare NaOH solution with a concentration of 10 mol/mL. Then 5.816 g $Ni(NO_3)_2 \cdot 6H_2O$ as Ni source were dissolved into 20 mL deionized water to obtain a dark green solution. After two solutions were prepared, the NaOH aqueous solution was added into the $Ni(NO_3)_2$

solution with a dropping speed of 0.5 mL/min while stirring. During the dripping procedure of NaOH solution, green colloidal precipitation was formed. The colloidal precipitation was suction filtrated and washed with deionized water for three times and dried in oven for 6 hours at 70 ℃. The obtained green dry matter was grinded thoroughly and calcined in Muffle furnace at 270 ℃ for 2 h. After that, a dark-black NiO_x powder was obtained. The 25 mg/mL NiO_x ink were obtained by dispersing NiO_x NPs into deionized water and ultrasonicating for 1 h.

Device fabrication:

Firstly, glass/ITO substrates were cleaned by an ultrasonic machine (KQ320DV) in mixed detergent composed of Decon 90 and deionized water with a volume ratio of 1:25, and then in deionized water for 5 times, 20 minutes for each time. After that, the substrates were dried by nitrogen flow. 30 μL NiO_x ink were spin coated on each dried ITO substrate at 400 rpm for 3 s and at 4000 rpm for 30 s sequentially and then annealed at 200 ℃ for half an hour. After that, the substrates were transferred into glovebox immediately. For BRS-NiO_x, 50 μL different concentration of AA (dissolved in DMF) were spun on NiO_x film at 400 rpm for 3 s and at 4000 rpm for 30 s in sequence, and then annealed on hot plate at 100 ℃ for 30 min. Next, 30 μL perovskite precursor solution were spun at 400 rpm for 3 s and at 6000 rpm for 40 s sequentially, 180 μL CB as anti-solvent were dropped instantly on the center of spinning substrates before the end of spin coating by 18 s. All the perovskite films were annealed at 50 ℃ for 2 min and then annealed at 85 ℃ for 30 min. Then 30 nm C_{60}, 7 nm BCP and 100 nm silver (Ag) electrodes were deposited in high vacuum condition sequentially using a shadow mask. The cell area was 0.0625 cm^2 defined by the crossing area between the ITO and Ag electrodes. Perovskite precursor solution was prepared in a mixed solvent composed

of DMF and DMSO with a volume ratio of 4:1. The molar ratio for (FAI/MAI) and (Pb/Sn) was 0.6/0.4 and the concentration was 1.8 M. Besides, SnF_2 (10% relative to SnI_2), $Pb(SCN)_2$ (10% relative to PbI_2), tin powder (with a concentration of 2.5 mg/mL) were added. After all of the components were mixed into solvent, perovskite precursor solution was stirred for 2 hours at room temperature and then filtered by a 0.22 μm PTFE membrane to get rid of remained tin powders.

Characterization

The absorbance and transmittance of films were measured by absorption spectrometer (Shimadzu UV-2450) and UV-Vis-NIR spectrophotometer (Agilent Technologies Cary Series), respectively. The field emission scanning electron microscopy (FESEM) morphologies of perovskite film were obtained by field emission scanning electron microscope (JSM-7800F). The X-ray diffraction (XRD) patterns of films were analyzed by XRD-7000 diffractometer with a step size of 0.4°. Transient photocurrent (TPC) of devices were measured with laser pulse (532 nm, 6 ns width from an Nd:YAG laser) and an input impedance of 50 Ω. The morphologies of NiO_x films were monitored by using atomic force microscope (AFM, CSPM 5500). The current density-voltage (J-V) characteristics of the solar cells were carried out in nitrogen-filled glovebox using a Newport 94043A solar simulator with 100 mW·cm-2 AM 1.5G simulated sunlight. The EQE was measured in nitrogen filled glovebox by using a Xenon arc lamp, a monochromatic instrument, and a lock-in amplifier. The X-ray photoelectron spectroscopy (XPS) measurements were performed by photoelectron spectrometer (ESCALAB 250Xi). The PL emission spectra and the time-resolved PL decay were tested by Edinburgh instrument FLS 1000, and the TRPL measurements were conducted using 405-nm picosecond pulsed laser, and fluorescence was detected

via a near-infrared detector. The FTIR spectra were recorded with a Nicolet iS50 Infrared Fourier transform microscope by Thermo Fisher Nicolet 6700.

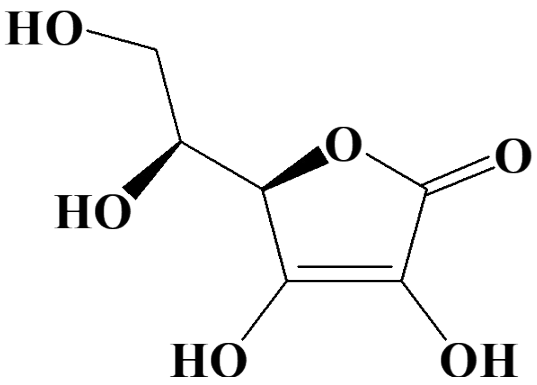

Fig. S1. The molecular formula of ascorbic acid (AA).

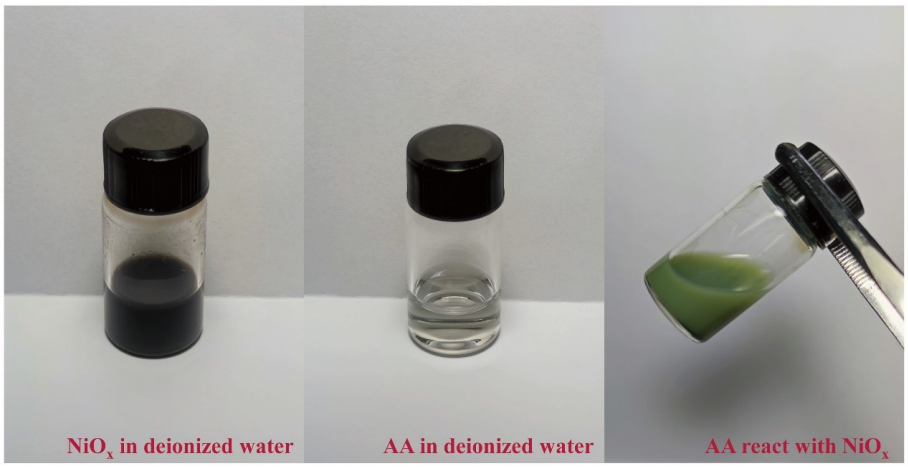

Fig. S2. NiO_x NPs react with AA.

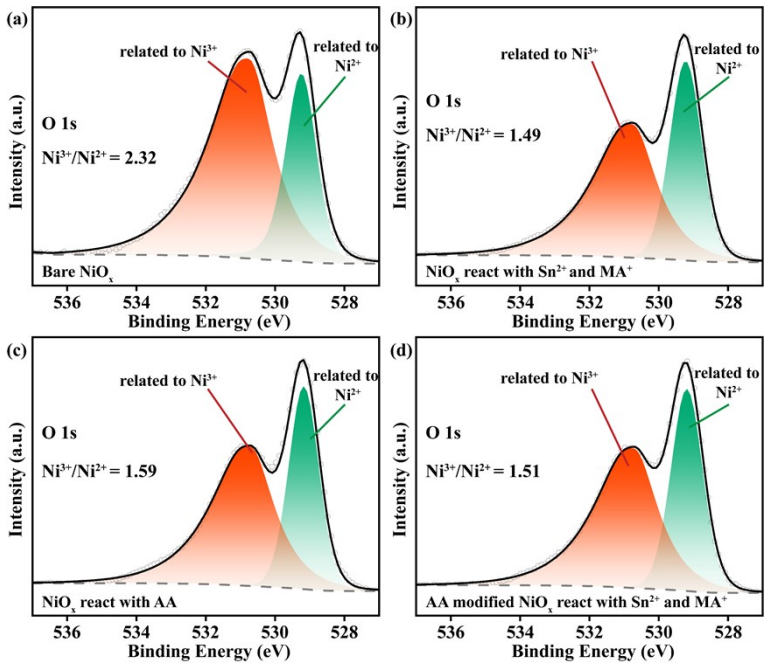

Fig. S3. O 1s high resolution XPS of (a) bare NiO_x reacted with (b) Sn^{2+} and MA^+, (c) AA, (d) reacted with AA and then reacted with Sn^{2+} and MA^+.

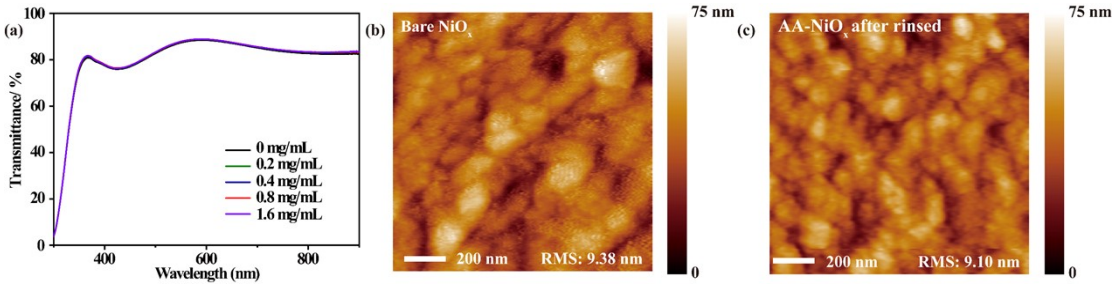

Fig. S4. (a) The transmittance of NiO_x treated with different concentrations of AA. The atomic force microscopy (AFM) images of (b) NiO_x and (c) Rinsed AA-NiO_x.

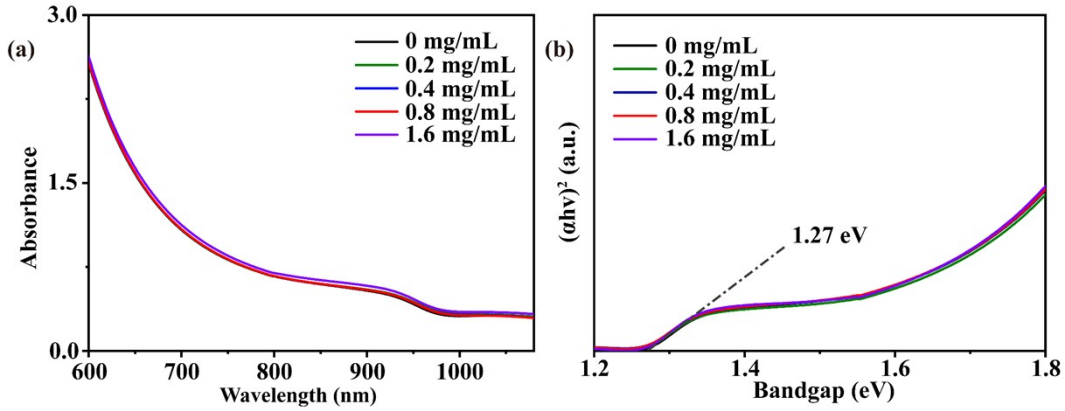

Fig. S5. (a) absorbance and (b) bandgap of NBG films deposited on NiO_x modified with different concentrations of AA.

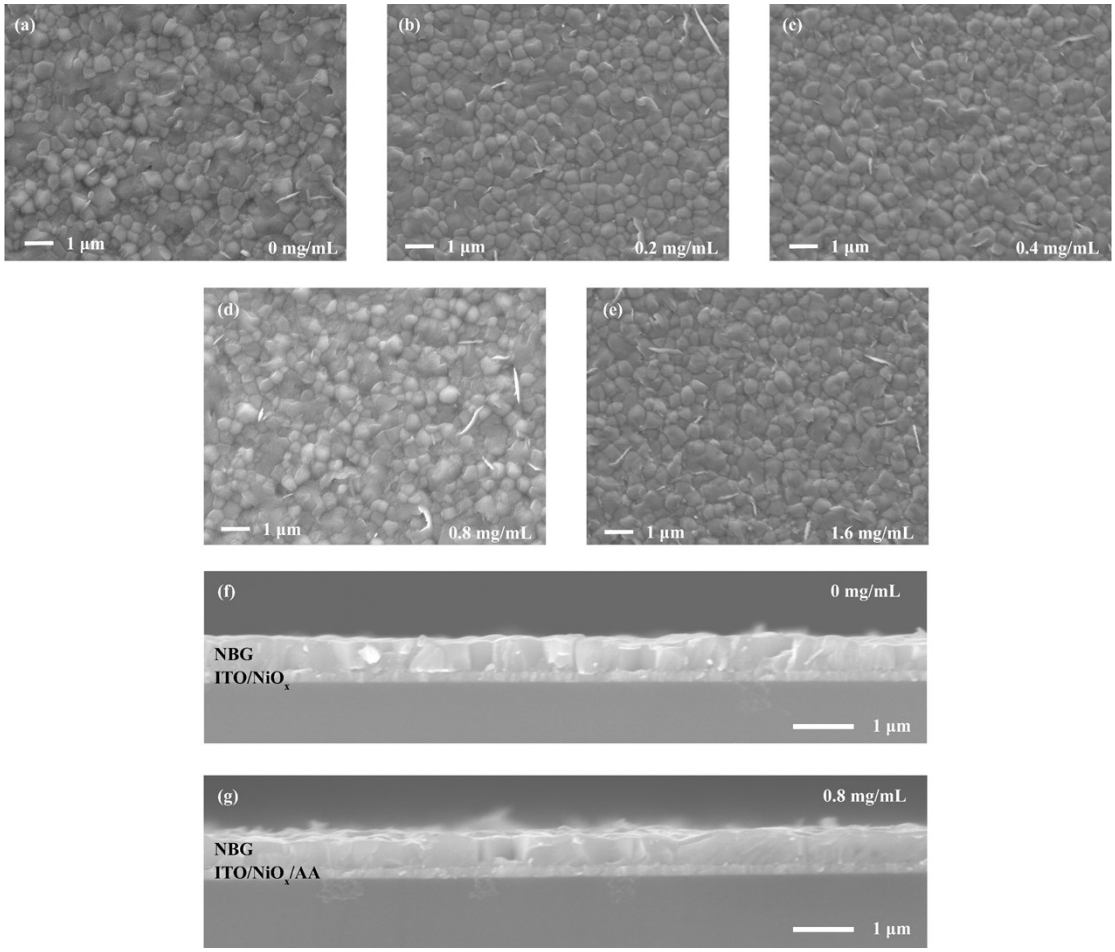

Fig. S6. (a-e) Top-view FESEM images of perovskite on NiO_x films treated by different concentrations of AA. (f-g) Cross-sectional FESEM images of perovskite on NiO_x films and on NiO_x treated by AA with 0.8 mg/mL.

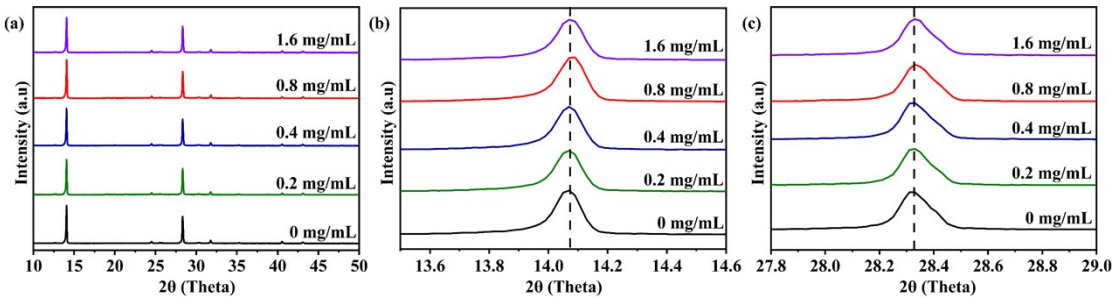

Fig. S7. (a) XRD patterns of NBG films deposited on NiOx films treated by various concentrations of AA. XRD patterns at (b) (110) plane preferred orientation and (c) (220) plane preferred orientation of perovskite films deposited on NiO_x treated with different AA concentrations.

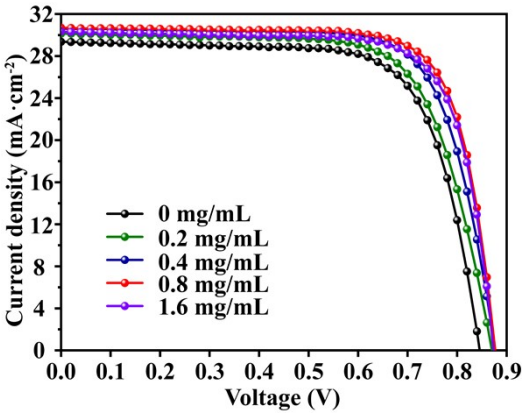

Fig. S8. *J-V* curves of champion devices with various AA concentrations modified on NiO_x.

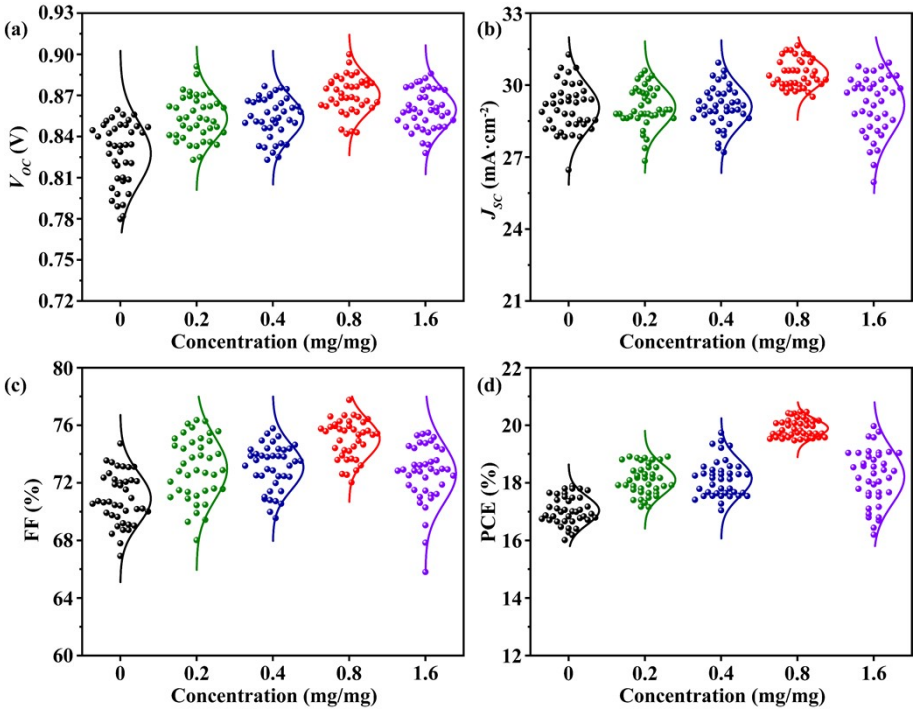

Fig. S9. The statistic performance of devices with different concentrations of AA on NiO_x.

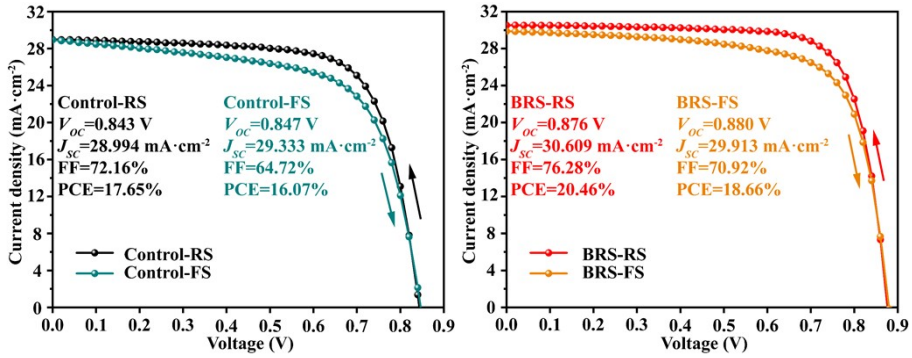

Fig. S10. The *J–V* curves of control and AA modified devices measured under forward and reverse voltage scans.

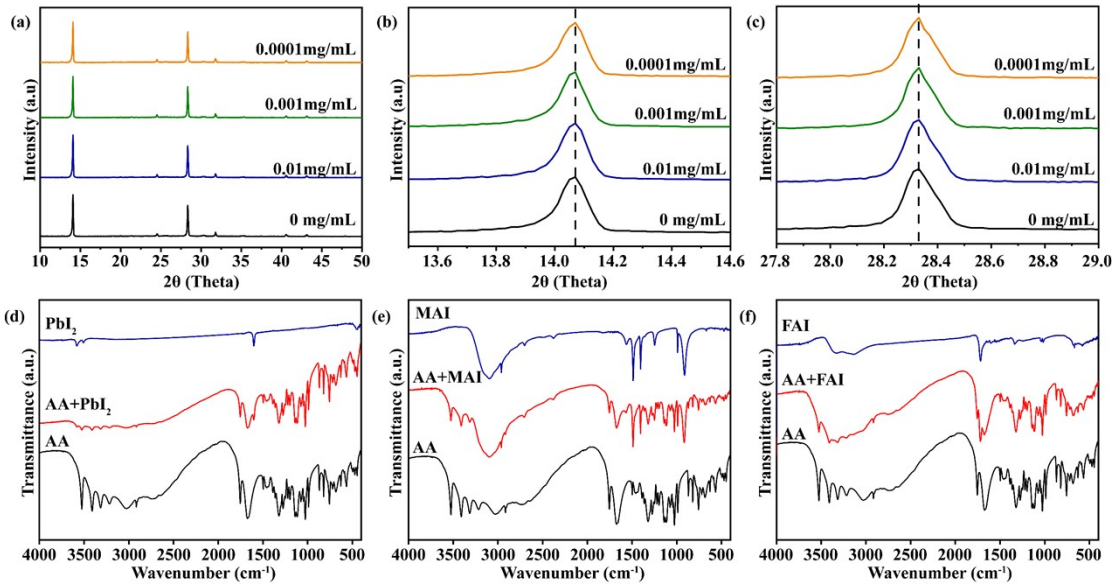

Fig. S11. (a-c) XRD patterns of perovskite films doped with different minor concentrations of AA. FTIR patterns of the interactions between AA and (d) PbI_2, (e) MAI, (f) FAI, respectively.

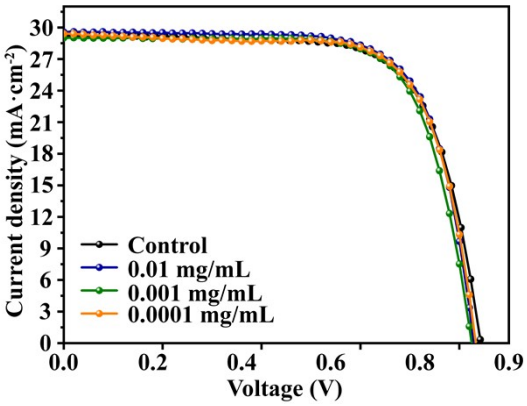

Fig. S12. The *J-V* curves of devices with different low concentrations of AA doped into perovskite.

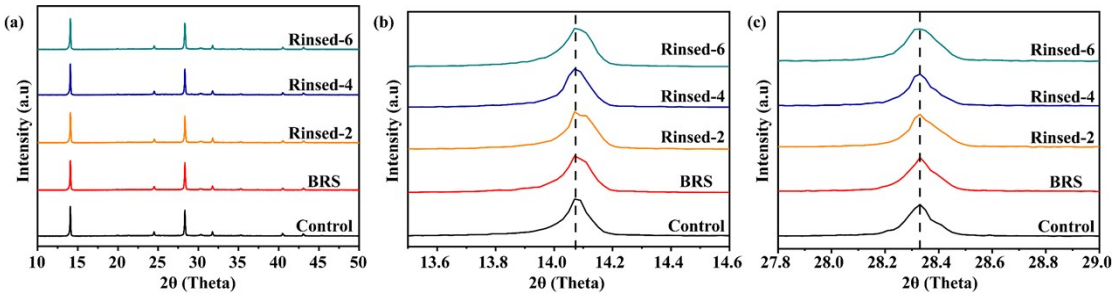

Fig. S13. XRD patterns of NBG perovskite films deposited on modified NiO_x which were rinsed by DMF with different times.

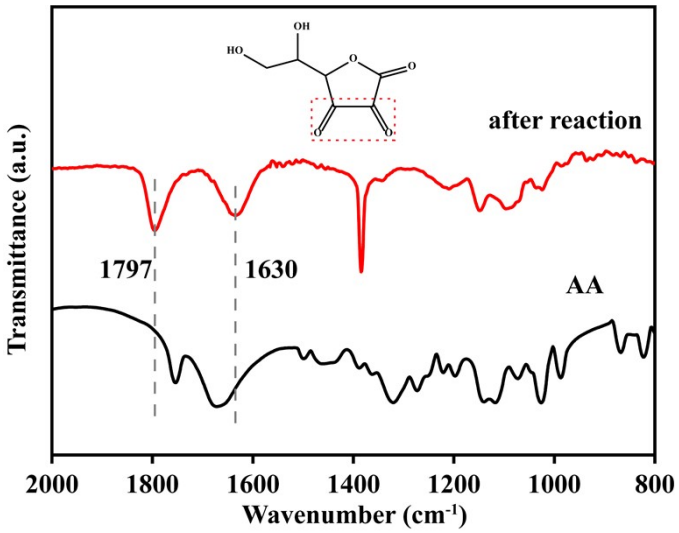

Fig. S14. FTIR pattern for AA and AA after reacted with NiOx. Two peaks at 1797 and 1630 cm^{-1} relevant to ν(C=O) in dehydroascorbic acid (oxidized form of AA) appeared.

Table S1. Statistics on photovoltaic parameters of PSCs.

Sample	V_{OC} (V)	J_{SC} (mA·cm^{-2})	FF (%)	PCE (%)
Control	0.828±0.023	29.059±0.975	70.907±1.763	17.038±0.486
BRS-0.2	0.853±0.016	29.089±0.831	72.991±2.136	18.107±0.516
BRS-0.4	0.854±0.015	29.105±0.839	73.079±1.554	18.156±0.634
BRS-0.8	0.870±0.014	30.467±0.587	75.063±1.350	19.896±0.310
BRS-1.6	0.860±0.014	29.175±1.212	72.636±2.036	18.212±0.943

Table S2. Device structures and photovoltaic parameters of the inverted NBG PSCs

Device structure	V_{OC} (V)	J_{SC} (mA·cm^{-2})	FF (%)	PCE (%)	Band gap (eV)	Year	Ref.
Glass/ITO/NiO_x/$FAPb_{0.75}Sn_{0.25}I_3$/PCBM/Ag	0.81	28.23	75.40	17.25	1.36	2018	1
Glass/ITO/NiO_x/$Cs_{0.1}MA_{0.2}FA_{0.7}Pb_{0.5}Sn_{0.5}I_3$/$C_{60}$/BCP/Ag	0.771	31.1	73.3	17.6	1.25	2019	2
Glass/ITO/L-NiO_x/$MA_{0.4}FA_{0.6}Pb_{0.4}Sn_{0.6}I_3$/PCBM/Ag	0.82	29.6	77.2	18.77	1.27	2021	3
Glass/ITO/NiO_x/PFN/$MA_{0.5}FA_{0.5}Pb_{0.5}Sn_{0.5}I_3$/$PC_{61}BM$/Ag	0.88	29.5	76	19.8	1.26	2021	4
Glass/ITO/E-NiO_x/$FA_{0.8}Cs_{0.2}Pb_{0.5}Sn_{0.5}I_3$/ALD-$SnO_2$/Cu	0.713	16.4	76.5	16.7	Not mentioned	2021	5
Glass/ITO/NiO_x/PTAA/HBA doped and vertical Compositional Gradient $FA_{0.5}EA_{0.05}MA_{0.45}Pb_{0.5}Sn_{0.5}I_3$/PCBM/BCP/Ag	0.88	31.36	79.78	22.02	1.25	2021	6
Glass/ITO/NiO_x/AA/$MA_{0.4}FA_{0.6}Pb_{0.4}Sn_{0.6}I_3$/$C_{60}$/BCP/Ag	0.877	30.62	76.27	20.48	1.27	2022	This work

Table S3. Photovoltaic parameters of PSCs on different scan directions.

	Scan direction	V_{OC} (V)	J_{SC} (mA • cm^{-2})	FF (%)	PCE (%)	Hysteresis Index
Control device	**reverse**	0.843	28.994	72.16	17.65	1.10
	forward	0.847	29.333	64.72	16.07	
BRS device	**reverse**	0.876	30.609	76.28	20.46	1.10
	forward	0.880	29.913	70.92	18.66	

Table S4. EIS fitted parameters of control and BRS devices.

Sample	R_s (Ω)	R_{rec} (Ω)
Control device	20.85	332
BRS device	34.05	1865

Table S5. Carrier lifetime and fitted parameters of perovskite thin films grown on bare NiO_x film and on BRS film.

Sample	τ_1 (ns)	τ_2 (ns)	τ_{ave} (ns)
Control	9.051	50.287	41.169
BRS	8.442	34.029	26.259

References

1 D. Chi, S. H. Huang, M. Y. Zhang, S. Q. Mu, Y. Zhao, Y. Chen and J. B. You, *Adv. Funct. Mater.*, 2018, **28**, 1804603.

2 Q. L. Han, Y. Wei, R. X. Lin, Z. M. Fang, K. Xiao, X. Luo, S. Gu, J. Zhu, L. M. Ding and H. R. Tan, *Sci. Bull.*, 2019, **64**, 1399-1401.

3 H. Chen, Z. J. Peng, K. M. Xu, Q. Wei, D. N. Yu, C. C. Han, H. S. Li and Z. J. Ning, Sci China Mater, 2021, **64**, 537-546.

4 X. Y. Hou, F. J. Li, X. Zhang, Y. F. Shi, Y. X. Du, J. B. Gong, X. D. Xiao, S. Q. Ren, X. Z. Zhao and Q. D. Tai, *Sol. RRL*, 2021, **5**, 2100287.

5 H. Gao, Q. W. Lu, K. Xiao, Q. L. Han, R. X. Lin, Z. Liu, H. J. Li, L. D. Li, X. Luo, Y. Gao, Y. R. Wang, J. Wen, Z. G. Zou, Y. Zhou and H. R. Tan, *Sol. RRL*, 2021, **5**, 2100814.

6 J. P. Cao, H. L. Loi, Y. Xu, X. Y. Guo, N. X. Wang, C. K. Liu, T. Y. Wang, H. Y. Cheng, Y. Zhu, M. G. Li, W. Y. Wong and F. Yan, *Adv. Mater.*, 2022, **34**, 2107729.